TANG, Rui; WANG, Shengwei; YAN, Chengchu. A direct load control strategy of centralized air-conditioning systems for building fast demand response to urgent requests of smart grids. Automation in Construction, 2018, 87: 74-83.
https://doi.org/10.1016/j.autcon.2017.12.012

A Direct Load Control Strategy of Centralized Air-conditioning Systems for Building Fast Demand Response to Urgent Requests of Smart Grids

Rui Tang[1], Shengwei Wang[1,2*] and Chengchu Yan[1]

[1] Department of Building Services Engineering, The Hong Kong Polytechnic University, Kowloon, Hong Kong

[2] Research Institute for Sustainable Urban Development, The Hong Kong Polytechnic University, Kowloon, Hong Kong

Abstract: When receiving an urgent request from a smart grid, shutting down part of operating chillers directly in the air-conditioning system in a building can achieve immediate power reduction. However, no study has addressed how to determine the number of chillers/pumps to be shut down and how to regulate the load of retained equipment systematically during DR events. This paper presents a new approach to address these issues based on three schemes. A power demand optimization scheme predicts the building cooling demand and the power limiting threshold in response to a received DR request. A system sequence control resetting scheme determines the number of operating chillers/pumps to be retained. An online control/regulation scheme ensures the system power following the expected profile by regulating the total chilled water flow delivered to the building and therefore the chiller load. It also employs a cooling distributor to distribute chilled water to individual zones concerning different sensitivities/sacrifices to temperature increases. Case studies are conducted on a simulated dynamic building air-conditioning system. Results show that, during DR events, the proposed strategy can achieve the expected power reduction (i.e., about 23%) and also maintain acceptable zone temperature even though uncertainties exist in the prediction process.

Keywords: direct load control, fast demand response, peak demand limiting, supply-based feedback control, smart grid

---

Corresponding author: Shengwei Wang, email: beswwang@polyu.edu.hk

1. Introduction

The power balance between the supply side and the demand side of a power grid is a critical issue in grid operation. However, the rapid growth of power demand and the integration of large amounts of renewable generation, which heavily depends on the weather conditions, impose a huge stress on the balance of the power grid [1-3]. Any power imbalance will cause severe consequences in the reliability and quality of power supply (e.g., voltage fluctuations and even power outrages) [4]. Facing the challenges from the power imbalance, the smart grid is considered as a very promoting solution to incorporate advanced technologies to offer better flexibility, reliability and security in grid operation. A smart grid improves the communication ability between power producers and consumers to make decisions about how and when to produce and consume electrical power [5]. The control of power demand at the consumer side in response to grid requests (e.g., dynamic price and reliability information) is known as demand response (DR) [6]. DR programmes can benefit power grids in reducing peak loads and hence avoid huge investments in upgrading the grids [7]. They can also provide considerable economic benefits for building owners [8, 9].

Among different kinds of consumers at the power demand side, buildings are one of the major energy consumers today and their share is increasing due to the urbanization. Considering the elastic nature of building energy use, the interaction between buildings and power grids could be very promising. Moreover, with the help of advanced technologies such as building automation systems and smart meters, demand response control strategies in buildings could be implemented to realize this bidirectional operation mode between buildings and power grids [10, 11]. Heating, ventilation, and air-conditioning (HVAC) systems, accounting for more than 50% of energy used in buildings in the USA [12], are excellent demand response resources to reduce or shift the electricity demand during peak periods [13].

Load shifting, which is the process of shifting on-peak loads to off-peak hours so as to take advantage of electricity rate difference in different periods, is more commonly-used for demand side management in commercial buildings. Many studies have been conducted on load shifting [14-17]. Xu and Haves [18] conducted a preliminary case study to demonstrate the potential of utilizing building thermal mass for peak demand reduction in an office building in California. Two precooling and zone temperature reset strategies were tested. The results pointed out that the limiting control strategy could reduce the chiller power significantly. Sun et al. [19] conducted case studies concerning the peak demand reduction to minimize energy cost and peak demand charge using an indoor air temperature set-point reset strategy that achieved significant power reduction on HVAC systems during peak hours. However, due to inevitable energy losses in the power charging and discharging processes, the peak load reduction is realized at the expense of increasing energy consumption. In addition, resetting the indoor air temperature cannot achieve significantly immediate power reduction within a very short time interval (i.e., minutes) resulting from the inherent and significant delay of charging and discharging control processes [20].

Facing urgent requests and incentives from smart grids, direct load control (DLC) is considered as an effective way to achieve immediate power reduction within a very short time. Direct load control means that electricity utilities have the permission to control (e.g., switch off) the specific devices/systems of end-users and give a certain incentive to them based on their previous agreements (e.g., contracts) [21, 22]. Many studies on DLC have been conducted, particularly for residential buildings. DLC is considered as an effective means to achieve power reduction and provide frequency regulation services [23, 24]. The frequency regulation services are used to deal with the grid imbalance from the viewpoint of power demand side, which also have the requirement on response time. The main objective of frequency regulation is to modify the power use on the demand side to match the power supply. The modulation required to provide frequency regulation cannot be achieved with residential cooling equipment that does not incorporate variable-speed drives for the refrigerant compressor motor. Moreover, DLC for frequency regulation makes economic sense for very small cooling systems.

In fact, the power demand of chillers accounts for a large part of power use in commercial buildings using centralized air-conditioning systems. When power grids need an immediate and significant power reduction on the demand side, shutting down some of operating chillers directly in a commercial building turns out to be effective, which is a typical DLC programme and has been applied in real projects in some areas. For example, in Hong Kong, the utility company, CLP, has recently launched a demand response programme, namely "Automated DR programme", which is actually a direct load control programme. With agreements in advance and devices installed at the customer side, part of operating chillers could be reduced by the utility company automatically and remotely when there is an urgent need in power reduction.

Although shutting down some of operating chillers in commercial buildings can achieve immediate power reduction, the operating states of air-conditioning systems are obviously changed. The authors of this paper pointed out that the unbalanced chilled water distribution in an air-conditioning system would occur after simply shutting down some of operating chillers [25]. A novel supply-based feedback control strategy based on adaptive utility function was developed and effectively solved this problem. However, no previous study was carried out on how to determine the number of chillers to be shut down during DR events from the viewpoint of whole air-conditioning systems. This is because shutting down part of operating chillers would significantly influence the power consumption of equipment other than chillers in an air-conditioning system. In addition, how to regulate the loads of retained equipment in a system to realize expected power limiting threshold is also needed to be discussed.

In this paper, a fast demand response control strategy concerning a typical air-conditioning system (i.e., constant water flow in the primary chilled-water loop and variable water flow in the secondary loop) is developed for proper system control responding to urgent requests from smart grids. The main innovations and original contributions of this research include: (1) a systematic approach is proposed to make such fast demand response method (i.e., shutting down part of operating chillers) effective for urgent requests of smart grids; (2) an power demand optimization scheme is developed to determine the power limiting threshold considering the indoor thermal environment; (3) a system sequence control resetting scheme is proposed to determine the numbers of retained devices in an air-conditioning system during a DR event; (4) an online control/regulation scheme is developed to maintain the system power demand at an expected power profile; (5) a modified cooling distributor is introduced concerning the uncertainty of prediction process. Case studies are conducted to test and validate the effectiveness and performance of this proposed control strategy.

2. Direct load control strategy

2.1 Overall structure and approach

Generally, the power demand of a commercial building is contributed by building services systems, including heating, ventilation and air-conditioning (HVAC) systems, lighting, electrical equipment, lifts and elevators, etc. The total power demand (i.e., electricity load) of a commercial building can be divided into two parts [26]: sheddable power demand and controllable power demand. Electricity loads of lighting, electrical equipment, transportation and other appliances are the sheddable power demands, which can be conveniently obtained according to their operation schedules. In contrast, the electricity loads of HVAC systems are the controllable power demands, which are possible to be altered by power demand controls. In this study, the power reduction of an air-conditioning system in a commercial building is concerned to meet the urgent requests of smart grids.

With a sudden pricing change or an urgent incentive given by a utility company during a DR event, the fast demand response control strategy is activated to realize immediate power reduction. In general, this control strategy implemented in real projects mainly consists of two steps: overall decision-making and control implementation. At the overall decision-making step, the numbers of devices to be shut down and the power limiting threshold are determined. At the control implementation step, the power demand of the air-conditioning system is adjusted to achieve the pre-determined power limiting target during a DR event after shutting down part of operating devices as determined.

The overall structure of the fast demand response control strategy is shown in Fig.1. It mainly includes the power demand optimization, the system sequence control resetting and the online control/regulation. Once a DR request is received, the baseline of building power demand predictor estimates the building cooling and power demand profiles in a normal condition. Then, the power demand optimization scheme is activated. Three models, determination of thermal comfort sacrifice, building cooling demand predictor and power demand predictor, are contained in this scheme. According to the urgent incentive, the sacrificed thermal comfort in terms of indoor air temperature increase is determined. The building cooling demand predictor predicts the reduced building cooling demand profile during the DR event based on the baseline of cooling demand and allowed indoor air temperature increase. And the power demand predictor is used to calculate the power limiting threshold during the DR event. Afterwards, the system sequence control resetting scheme resets the numbers of operating devices (i.e., chillers and pumps) to be retained based on the reduced building cooling demand. The fan speed is also set by this scheme and all of these sequence control settings will remain to be unchanged during the entire DR period. Finally, the online control/regulation scheme is to modulate the system power demand following the power limiting threshold as well as to realize a proper cooling allocation during the DR event. In this scheme, the chiller load regulator is used to achieve the former objective by fine-tuning the chilled water flow delivered to the building (i.e., adjusted cooling supply). The cooling distributor, which is based on the supply-based feedback control strategy, is employed to distribute the adjusted cooling supply to each zone properly and reasonably.

If utility companies shut down/control the chillers and corresponding devices in an air-conditioning system when an urgent DR request is given by smart grids, this fast demand response control strategy would be a direct load control strategy. In addition, this fast demand response method can be put into smart meters and activated by building owners responding to a sudden price change or incentive in order to achieve a bidirectional operation mode between buildings and smart grids. Although this study is focused on the DLC, Fig.1 is willing to provide wider applications for smart grids.

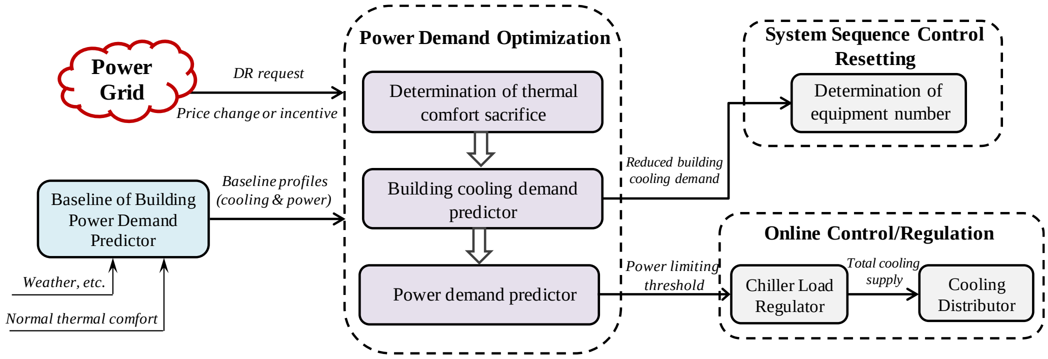

Fig.1 Basic approach of fast demand response control strategy during DR events

The above schemes of power demand optimization, system sequence control resetting and online control/regulation are introduced in detail in the following sections. The baselines of building cooling and power demands are assumed to be known, which have been carried out in many previous studies and are not the focus in this study.

2.2 Power demand optimization

This scheme includes three parts, i.e., determination of thermal comfort sacrifice, building cooling demand predictor and power demand predictor.

Determination of thermal comfort sacrifice

In this study, the indoor thermal comfort is represented by the indoor air temperature. The relationship between the incentive given by the utility company and the indoor air temperature sacrifice accepted by the end-users is shown in Fig.2. The general trend is that the more incentive provided, the more indoor air temperature increase accepted. But as the incentive increases, the change rate of the profile would decrease. This profile can be obtained by subjective surveys and not the main focus of this study. So the maximum acceptable indoor air temperature increase during the DR event is assumed to be 3°C in this study.

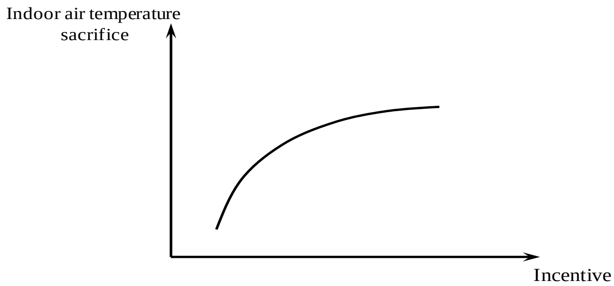

Fig.2 Relationship between incentive and indoor air temperature sacrifice

Building cooling demand predictor

This predictor is developed to predict the building cooling demand under the increased indoor air temperature as determined during the DR event. The building cooling demand during the DR event will be less than the baseline of normal case since certain numbers of operating chillers are shut down. A simplified building thermal storage model [26], which can represent the thermal characteristics and the building cooling demand reduction potentials, is used to estimate the influence of thermal mass on the building cooling demand.

The building cooling demand (Q_{dem}^{k}) at k^{th} time step during the DR event is calculated by Eq.(1).

$$Q_{dem}^{k} = Q_{base}^{k} - \Delta Q_{dem}^{k} \quad (1)$$

where, Q_{base}^{k} is the building cooling demand at k^{th} time step in the baseline case. ΔQ_{dem}^{k} is the predicted building cooling demand reduction at k^{th} time step.

Eq.(2) describes the relationship between the indoor air temperature increase and building cooling demand reduction [27]. ΔQ_{bui}^{k} is the cooling discharged by the thermal mass, while the later part in Eq.(2) is used to calculate the cooling discharged by the indoor air.

$$\Delta Q_{dem}^{k} = \Delta Q_{bui}^{k} + C_{in} * (dT_{in}/dt) * M_{air} \quad (2)$$

where, ΔQ_{bui}^{k} is the discharge cooling of the building thermal mass (i.e., the passive thermal storage), as calculated by Eq.(3). C_{in} is the specific heat of indoor air. M_{air} is the mass of indoor air. dT_{in}/dt is the increase rate of indoor air temperature after shutting down part of operating chillers. The indoor air temperature is assumed to reach the limit value in half an hour with a constant rate during the DR event. The objective of this assumption is for the simplicity in calculating the cooling released by the indoor air when its temperature increases. There are two reasons to do this assumption: first, the DR event in this study is set as two hours and the second hour would be the critical period when the indoor air temperature increases to the maximum value after shutting down part of operating chillers. The indoor air will discharge cooling as the result of the temperature increase, which reduces the cooling demand (lower than the original). The indoor temperature is assumed to reach the limit in 30 minutes so that the cooling discharged by the indoor air is released completely during the first 30 minutes of the DR event. Consequently, this would lead to underestimate the cooling demand in the first half an hour when the indoor air temperature is still below the temperature limit (27°C in this study). In contrast, this assumption would overestimate the cooling demand after the first half an hour of the DR event in order to ensure the indoor temperature acceptable particularly during this critical period. Secondly, this assumption is also benefited by the fact that during a DR event, temperature increase rate (i.e., $\mathrm{dT_{in}/dt}$) would decrease along with the time and the influence of the second part in Eq.(2) on building cooling demand alternation would be reduced accordingly. Generally, this assumption can be considered as a method to ensure the indoor temperature within the acceptable range and also make the prediction simple and convenient.

ΔQ_{bui}^{k} is calculated using a simplified building thermal storage model, as shown in Eq.(3) [26].

$$\Delta Q_{bui}^{k} = \frac{T_{in}^{k} - T_{base}^{k}}{R_{bui,o} + R_{bui,i}} * \left(1 + \mu * e^{-\frac{t}{\tau}}\right) * A_{bui} \quad (3)$$

$$\tau = \frac{R_{bui,o} * R_{bui,i}}{R_{bui,o} + R_{bui,i}} * C_{bui} \quad (4)$$

$$\mu = \frac{R_{bui,o}}{R_{bui,i}} \quad (5)$$

where, T_{base}^{k} is the indoor air temperature in the normal case (i.e., baseline). A_{bui} is the effective building surface area involved in the heat exchange process. τ is the time constant of building thermal mass and is defined in Eq.(4) [26]. μ is the ratio of the building outer thermal mass resistance to the building inner resistance as shown in Eq.(5) [26]. C_{bui} is the building thermal capacitance of per square meter. $R_{bui,o}$ and $R_{bui,i}$ are the building outer and inner thermal mass resistances, respectively.

Power demand predictor

This predictor is used to predict the building power demand during a DR event. In general, the building power demand is mainly consumed by building services systems including HVAC systems, lighting, electrical equipment, lifts and elevators, etc. In this study, the proposed direct load control focuses on the air-conditioning system to meet the request (i.e., immediate power reduction) from a smart grid and the power demands of the other parts are assumed to be unchanged with the baseline profiles, as shown in Eq.(6). The power demand of cooling tower is also assumed to be unchanged with the baseline profile as its power consumption accounts for a small part of power demand in an air conditioning system and could be ignorable compared with the other devices. Therefore, the power reduction realized by the DLC strategy is contributed by four parts including chillers, primary pumps, secondary pumps and fans. The power limiting threshold in a DR period is shown in Eq.(7) and the unchanged parts are not included.

$$P_{thr,bui}^{k} = P_{ac}^{k} + P_{other}^{k} \quad (6)$$

$$P_{thr}^{k} = P_{ch}^{k} + P_{pri}^{k} + P_{sec}^{k} + P_{fan}^{k} \quad (7)$$

where, $P_{thr,bui}^{k}$ is the building power limiting threshold at k^{th} time step during the DR event. P_{thr}^{k} is the considered power limiting threshold of an air-conditioning system (except the cooling tower fans) in this study. P_{ac}^{k}, P_{ch}^{k}, P_{pri}^{k}, P_{sec}^{k}, P_{fan}^{k} are the power demands of the air-conditioning, the chiller, the primary pump, the secondary pump and the fan at k^{th} time step, respectively. The calculations on the power demands, i.e., P_{ch}^{k}, P_{pri}^{k}, P_{sec}^{k}, P_{fan}^{k} are shown as follows:

(1) Power demand of chillers

The power demand of chillers is determined by the cooling demand (Q_{dem}^{k}) and *COP* (coefficient of performance), as shown in Eq.(8) [27]. The chiller's *COP* can be calculated by Eq.(9)-(10).

$$P_{ch}^{k} = Q_{dem}^{k}/COP^{k} \quad (8)$$

$$COP^{k} = a_4 * (PLR^{k})^4 + a_3 * (PLR^{k})^3 + a_2 * (PLR^{k})^2 + a_1 * (PLR^{k})^1 + a_0 \quad (9)$$

$$PLR^{k} = Q_{dem}^{k}/Q_{rated} \quad (10)$$

where, a_0--a_4 are the coefficients identified with the historic recorded data. Q_{rated} is the rated cooling capacity of the chiller. PLR^{k} is the part load ratio of the chiller at k^{th} time step during a DR event, which is calculated by Eq.(10).

(2) Power demand of primary pumps

For the primary constant-secondary variable chilled water system, the power demand of primary pumps is only determined by the operating number and the rated power, as illustrated in Eq.(11).

$$P_{pri}^{k} = N_{pri} * P_{rated} \tag{11}$$

where, P_{rated} is the rated power of the primary pumps. N_{pri} is the operating number of primary pumps during the DR period.

(3) Power demand of secondary pumps

The secondary pumps are variable speed pumps and their power demands depend on the pressure drop (H_{pu}), the water flow rate (M_{sec}) and the efficiency (η), as illustrated by Eq.(12) [28]. In ref.[29], three control methods are introduced for determining the pressure head of secondary pumps. In this study, the pressure head of the secondary pumps is controlled by a constant pressure difference in the remote loop. Thus, the total pressure head of the secondary pumps (H_{pu}) is computed by Eq.(13).

$$P_{sec}^{k} = \frac{M_{sec}^{k} * H_{pu}^{k}}{\eta^{k}} \tag{12}$$

$$H_{pu}^{k} = p_{con} + \beta * (M_{sec}^{k})^{2} \tag{13}$$

where, p_{con} is the set-point of pressure difference in the remote loop. m_{sec}^{k} is the flow rate in the secondary loop at k^{th} time step during the DR event. β is a coefficient training by the history data.

The efficiency of variable speed pump is gained using a polynomial approximation [30]. The characteristic of efficiency is based on the manufacturers' data at the full speed operation and can be extended to the variable speed operation using the pump affinity law. It is modeled using Eq.(14), which is a function of the fraction of the nominal flow [31].

$$\eta^{k} = \eta_{design} * [d_0 + d_1 * x^{k} + d_2 * (x^{k})^{2} + d_3 * (x^{k})^{3}] \tag{14}$$

where, η_{design} is the design pump efficiency. x^k is the fraction of nominal flow at k^{th}

time step during the DR event. d_0-d_3 are the coefficients identified with the historic recorded data.

The water flow rate in the secondary loop is determined by the building cooling load and the temperature difference of the chilled water system as shown in Eq. (15)

$$M_{sec}^{k} = Q_{dem}^{k}/(c_p * \Delta T^{k}) \tag{15}$$

where, C_p is the specific heat of the chilled water. ΔT^k is the temperature difference between supply and return chilled water in the secondary loop. This value (ΔT^k) is set as a constant value, i.e., 5℃. During the DR event, due to the limited cooling supply, this temperature difference would be a little larger than 5℃. Thus, the chilled water flow and the power demand of secondary pumps would be overestimated. But the overestimated power demand can be considered as a safety yield to avoid the indoor air temperature exceeding the acceptable range in the real operation.

(4) Power demand of air delivery fans

Similarly, the power consumption of the variable speed fans depends on the fan-delivered static pressure (Δp_{fan}), the air volume flow rate (V) and the efficiency (η_{fan}), as illustrated by Eq.(16) [32]. During the DR event, the total supply air flow (V^k) is maintained at nearly the same value as that just before the DR event. Otherwise, each fan would operate at its maximum power and reduce the effectiveness of the DR control [25]. The fan-delivered static pressure (Δp_{fan}) is determined by two components, as calculated by Eq.(17) [32]. The first part is the pressure head on the VAV air distribution system after the static pressure control sensor (P_{set}), which is controlled at a constant value in this study. The second part is the pressure loss across the rest of the VAV supply system, i.e., filters, coil, duct, etc., which is proportional to the square of the volume flow rate. The characteristic of efficiency (η_{fan}) is based on the manufacturers' data at the full speed operation and extended to the variable speed operation using the affinity law, as shown in Eq.(18).

$$P_{fan}^{k} = \frac{V^{k} * \Delta p_{fan}^{k}}{\eta_{fan}^{k}} \quad (16)$$

$$\Delta P_{fan}^{k} = P_{set} + \gamma * V^{2} \quad (17)$$

$$\eta_{fan}^{k} = \eta_{design,fan} * [e_0 + e_1 * x^{k} + e_2 * (x^{k})^2 + e_3 * (x^{k})^3] \quad (18)$$

where, γ, e_0-e_3 are coefficients training by the history data.

In this study, the baseline profile is assumed to be known. When the power limiting threshold is predicted, the power reduction is equal to the difference between the predicted power limiting threshold and the baseline profile, as computed by Eq.(19).

$$\Delta P_{thr}^{k} = P_{base}^{k} - P_{thr}^{k} \quad (19)$$

where, ΔP_{thr}^{k} is the predicted power reduction threshold during the DR event. P_{base}^{k} is the baseline profile of the system power demand.

2.3 Scheme of online control/regulation

As shown in Fig.3, the scheme of online control/regulation includes chiller load regulator and cooling distributor. The chiller load regulator ensures the measured system power demand following the power limiting threshold by adjusting the set-point of chilled water flow rate in the secondary loop. After the chiller load regulator, the cooling distributor distributes the cooling supply (i.e., total chilled water flow rate) among individual zones based on their demands. For a single AHU, a flow meter is used to measure its water flow, and the AHU coil valve is used to adjust the desired water flow from “cooling distributor”. The speed of secondary pumps is controlled to follow the “DP” (i.e., pressure set-point in the remote zone). In this implementation, one AHU serves a single thermal zone.

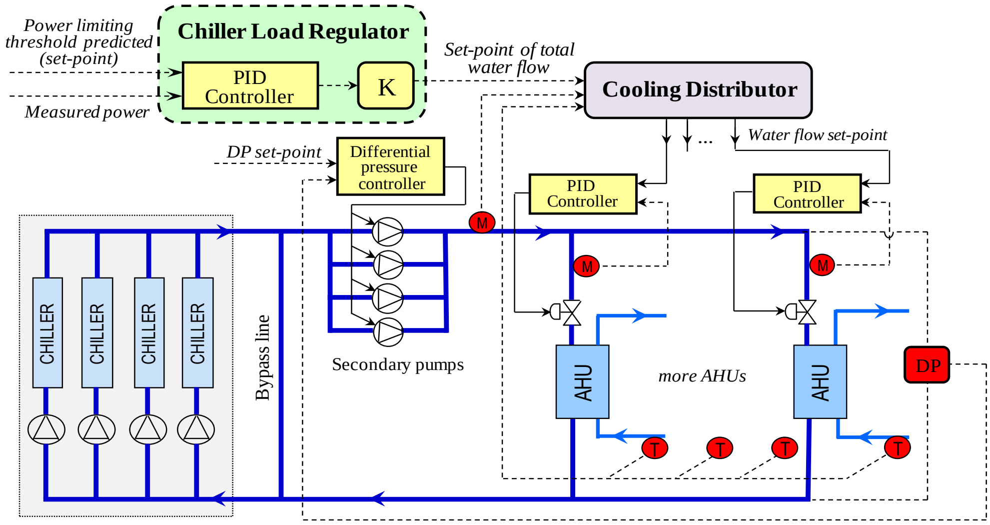

Fig.3 Schematic of online control/regulation during a DR event

Chiller load regulator

The control objective of the chiller load regulator is to ensure the total power consumption of an air-conditioning system following the power limiting threshold during a DR event. The control variable is the chilled water flow rate in the secondary loop. With the predicted power limiting threshold and measured power demand, a PID controller followed by an amplification factor is employed to realize the function of the chiller load regulator, as shown in Fig.3. The output of the chiller load regulator is the set-point of the total chilled water flow rate delivered to the building.

Cooling distributor

Due to the reduced number of operating chillers during the DR event, as will be determined in this section, the cooling supply is not sufficient to satisfy the cooling demand of end-users. This would lead to some inherent system operation problems (i.e., excessive speeding of chilled water pumps and air delivery fans, imbalanced chilled water distribution among AHUs, and imbalanced air distribution among VAV (variable air volume) terminals) if the air-conditioning system is still controlled by the conventional feedback control strategies. These serious problems will result in large temperature differences among different air-conditioned spaces, and also cause extra power consumption which obviously reduces the effect of the DR control. Thus, the cooling distributor based on supply-based feedback control instead of conventional control strategies is employed during the DR event [33].

Based on the method in ref.[25], an improved cooling distributor is developed. A factor representing the sensitivity of thermal comfort to the indoor air temperature increase is supplemented into the adaptive utility function. This modification makes cooling distribution more reasonable for real applications where different users have different levels of acceptable indoor air temperature sacrifice, as shown in Eq.(20).

$$U_i = 1 - \frac{|T_i - T_{set,i}|}{\theta * T_{band}} \qquad U_i \in [0,1] \qquad (20)$$

where, θ is a factor representing the sensitivity of the utility value to indoor air temperature increase. U_i is the utility value of i^{th} zone, which describes the occupant's satisfactory of thermal comfort in terms of indoor air temperature during the DR event. T_i is the measured indoor air temperature of i^{th} zone. $T_{set,i}$ is the original set-point (i.e., 24°C in this study) of indoor air temperature in the normal condition. T_{band} is a deviation between T_i and $T_{set,i}$, which should be large enough to fully cover the whole possible indoor temperature range during the DR event. Its value is set as 10°C in this study.

The basic mechanism in managing the distribution among n zones is that: generally, n zones should reach a uniform target value of thermal comfort index constrained by the total cooling resource provided. Compared with the target value, the cooling allocated to the zones with lower thermal comfort indexes should be increased while the cooling allocated to the zones with higher thermal comfort indexes should be reduced. The change of cooling to each zone is determined by the difference between the target value and the current value of its thermal comfort index (i.e., ΔU). The detailed description of the method can be found in [25]. The online calculation process of the cooling distributor is shown in Eqs.(21)-(23) [25].

$$M_{set,i}^{k} = M_{i}^{k} + \sqrt{\frac{1-U_{i}^{k}}{a_{i}}} \quad (21)$$

$$M_{set,i}^{k} = \lambda M_{set,i}^{k-1} + (1-\lambda) M_{set,i}^{k} \quad (22)$$

$$M_{sp,i}^{k} = M_{set,i}^{k} - \sqrt{\frac{1-\bar{U}_{sp}^{k}}{a_{i}}} \quad (23)$$

$$a_{i} = \frac{\Delta T_{i}}{T_{band} \times \Delta M_{i}^{2}} \quad (24)$$

$$\Delta T_{i} = (T_{out,i} - T_{set,i}) + 5 \quad (25)$$

where, M_i^k is the chilled water flow rate supplied to i^{th} zone at k^{th} time step. $M_{set,i}^k$ is a fictitious reference value of the water flow rate which is required to maintain the indoor air temperature at its original set-point before a DR event but under current cooling load condition. $\bar{U}_{sp}^{k}$ is the target utility value of all zones at k^{th} time step, which is determined by the total cooling supply. λ is the forgetting factor selected to be 0.95 in this study. $M_{sp,i}^k$ is the chilled water flow rate set-point for each zone. a_i is a parameter representing the thermodynamic characteristic of i^{th} zone, which is determined by the Eqs.(24-25) [33]. To determine the parameter a, ΔT_i is the indoor air temperature rise (stabilized) of i^{th} zone when the air-conditioning system is shut down. ΔM_i is the chilled water flow rate just before shutting down the air-conditioning system. To have a better reliability and simplify the identification process, the system design data are used. For identifying 'a_i', when the air-conditioning system is working, the indoor air temperature is assumed to be its design value. When the air-conditioning system is off, the indoor air temperature is assumed to be 5℃ higher than the design outdoor air temperature. Then, ΔT_i can be calculated by Eq.(25).

2.4 System sequence control resetting

The system sequence control resetting scheme is proposed to determine the number of retained chillers, the number of retained (primary and secondary) pumps and the fan speed setting during the DR event. These settings should be unchanged after implementation during the entire DR period.

The number of retained chillers is determined by the predicted cooling demand after indoor air temperature increases, as calculated by Eq.(26). Similar to the normal operation, the retained chillers should meet the maximum cooling demand during the DR event.

$$N_{ch} = ceil\,(\frac{Q_{dem}}{Q_{rated}}) \tag{26}$$

$$Q_{dem} = max(Q_{dem}^{k}) \tag{27}$$

where, N_{ch} is the number of retained chillers during the DR event. Q_{dem}^{k}, Q_{dem} are the cooling demand at k^{th} time step and the maximum value during the DR event, respectively. Q_{rated} is the rated cooling capacity of chiller. *ceil* is a function to round a number to the nearest integer toward positive infinite.

The concerned system is a typical primary constant-secondary variable chilled water system and each chiller is served by one corresponding primary pump. The number of retained primary pumps, therefore, would follow the number change of chillers, as shown in Eq.(28).

$$N_{pri} = N_{ch} \tag{28}$$

where, N_{pri} is the number of the retained operating primary pumps during the DR event.

The secondary pumps are responsible for transporting the cooling provided by chillers to end-users. The number of secondary pumps is determined based on the cooling demand represented by the required chilled water flow rate during the DR event, as shown in Eq.(29). The maximum value of chilled water flow rate during the DR period is used to determine the number of retained secondary pumps.

$$N_{sec} = ceil\ (M_{sec}/M_{rated}) \quad (29)$$

$$M_{sec} = max\ (M_{sec}^{k}) \quad (30)$$

where, N_{sec} is the number of the operating secondary pumps to be retained during a DR event. M_{sec}^{k} and M_{sec} are the required chilled water flow delivered to end-users at k^{th} time step and the maximum value during the DR event, respectively. M_{rated} is the rated water flow rate of secondary pump.

During the DR event, the AHU fans would operate at their full speeds after shutting down part of operating chillers. This is because the cooling supply could not maintain the indoor air temperatures at their original set-points and hence the dampers of VAV boxes are fully opened. The fully operating fans would seriously increase the system power consumption and obviously offset the power reduction contributed by the DR control. To avoid this phenomenon, the total supply air flow rate of each AHU is set as nearly the same as that just before the DR event.

In addition, the period right after the DR event is called power rebound (PR) period. During this period, the power demand is rather high because the system requires large amounts of power to resume back to its original condition quickly. Although there is no need to achieve a certain power reduction during the PR period, it is definitely not expected to impose a heavy stress on the power grid. In order to avoid serious power rebound phenomenon, a simple power limiting method is used. The indoor temperature is within the acceptable range although such power limiting method would reduce the recovery speed. During power rebound period, the same number of chillers as that just before the DR event is set to be operated at full capacity and the cooling distributors are still used to distribute the cooling supply as well. The fans are kept at the same operating condition as that during the DR event. These control settings are not released until the indoor air temperatures recover to their set-points.

3. Test platform

Computer-based simulation is an effective means to test and validate the proposed strategy in a commercial building integrated with a smart grid. A virtual test platform is built to test the fast demand response control strategy using dynamic models developed in TRNSYS [34]. The models used are validated by real data [35]. This test platform employs detailed physical models including the building envelop and major components (e.g. chillers, pumps, fans, hydraulic network, air ducts, AHUs) of a centralized air-conditioning system. The dynamic processes of heat transfer, hydraulic characteristics, water flow and air flow balance schemes (i.e., cooling distributor, developed by FORTRAN), energy conservation and controls among the whole system are simulated.

The central chiller plant simulated in this study is a typical primary constant-secondary variable chilled water system. It consists of six identical chillers with rated capacity of 4080 kW each and four secondary water pumps. The building is a super high-rise commercial building simulated by a multi-zone model (Type 56) in TRNSYS. Six air-conditioned zones with different cooling load profiles cooled by six AHUs are selected to test the proposed direct load control (DLC) strategy. Each zone consists of a VAV system served by one AHU, which includes a supply and a return fan with rated capacity 34 kW and 32 kW, respectively. The design supply air static pressure is 650Pa and fresh air flow set-point of a zone is set as constant according to the ASHRAE Standard 62.1-2013.

The office hour of the building is between 08:00am and 18:00pm and the DR period for test is between 14:00pm and 16:00pm in a typical summer day in Hong Kong. The outdoor weather condition in this day is shown in Fig.4. The original indoor air temperature set-point in normal condition is set to be 24℃. In the test, four chillers associated with four operating primary pumps are operating before the beginning of the DR event.

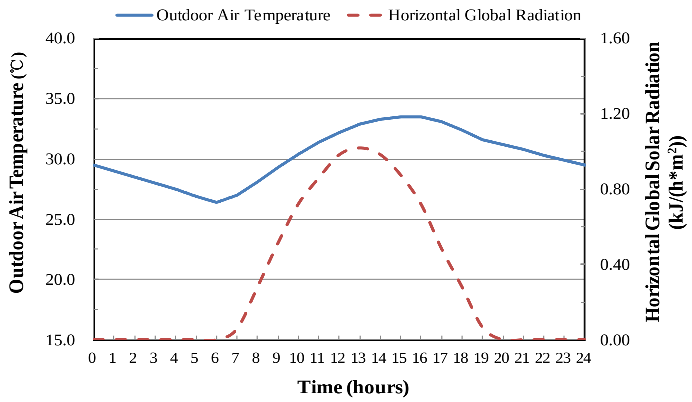

Fig.4 Weather condition of the test day

4. Results and discussion

4.1 System cooling demand and system sequence control resetting

The system cooling demand and determined operating numbers of chillers and pumps during the DR event are shown in Fig.5. As mentioned above, the maximum indoor air temperature sacrifice was assumed to be 3℃ in this study and the indoor air temperature limit was 27℃ during the DR event accordingly. In Fig.5, the cooling demand during the DR event was estimated using the building cooling demand predictor. Then the predicted cooling demand was used to determine the system sequence control settings. One of the four operating chillers was shut down and the same number setting was conducted for the primary pumps at the start of the DR event. Simultaneously, two of the four operating secondary pumps were also shut down at the start of the DR event.

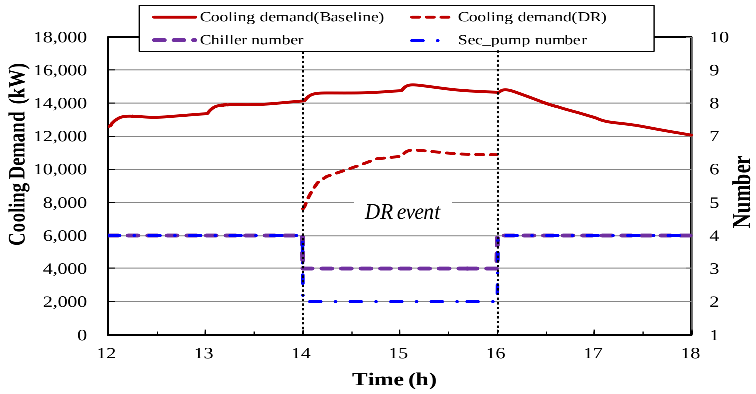

Fig.5 System cooling demand and determined operating numbers of chillers and pumps during the DR event

4.2 Power consumption of the air-conditioning system

As shown in Fig.6, the difference between the power baseline and the power limiting threshold was the achievable power reduction using the DLC strategy during the DR event. Using the chiller load regulator, the power consumption of the air-conditioning system could well track the command of the power limiting threshold during the DR event. Using the proposed DLC strategy, nearly 23% of power reduction (1100kW) could be realized immediately at the very beginning of the DR event. In addition, after the DR event, the power rebound condition, which may impose a heavy stress on the power grids after the DR period, was also improved significantly using the simple power limiting method. By limiting the number of operating chillers and the speeds of secondary pumps and air delivery fans during power rebound period, nearly 3000 kW (34%) power demand could be reduced compared to the power rebound profile (without power limiting).

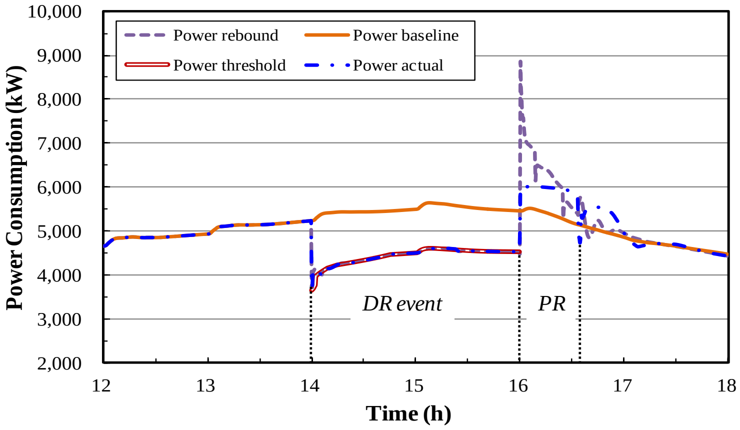

Fig.6 Power consumption of the air-conditioning system during the DR event

During the DR event, the power reduction was mainly achieved by the chillers and (primary and secondary) pumps, as shown in Fig.7. In contrast, the power reduction of AHU fans was relatively small because the setting of each air delivery fan was set to deliver the similar total air flow with that just before the DR event. During the power rebound period, the power demands of the operating chillers and the (primary and secondary) pumps were increased, while the power demand of the fans was still kept at the similar level with that during the DR event. Right after the PR period, each power demand profile in Fig.7 experienced an obvious fluctuation. This was because the air-conditioning system resumed to the original condition (i.e., indoor air temperature was 24℃) and the developed DLC strategy was switched to the conventional control strategy.

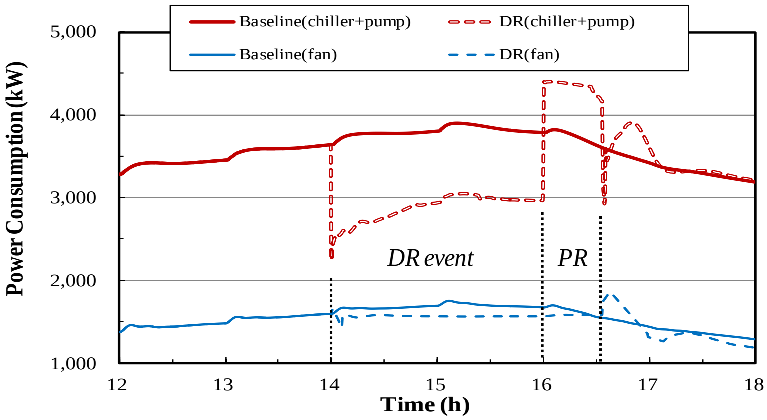

Fig.7 Power demands of chilled water system and fans during the DR event

Fig.8 presents the predicted and actual power reduction realized by the DLC strategy during the DR event. The average power reduction during the DR event was about 1100 kW. At the start of the DR event, the power reduction was slightly higher than the average value, which was mainly because the cooling stored in the building thermal mass was discharged. During the power rebound period, the achievable power reduction was negative, which meant that more power was consumed compared with the baseline profile in order to make the air-conditioning system resume to the original condition.

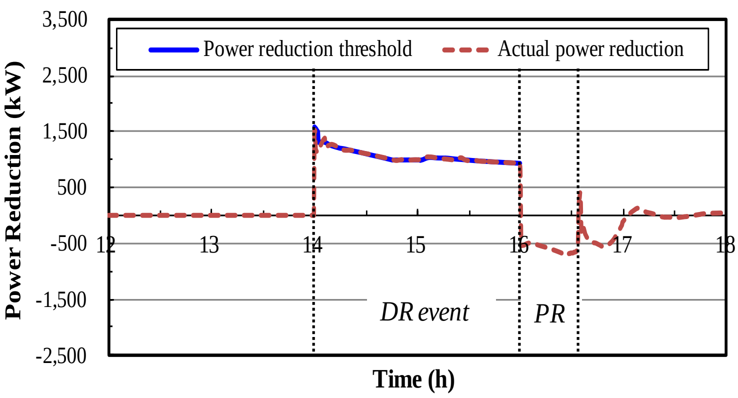

Fig.8 Power reduction of an air-conditioning system during the DR event

4.3 The indoor air temperatures of individual zones

As mentioned in section 2.3, by introducing the sensitivity factor, the improved cooling distributor can properly distribute the total chilled water among individual zones considering their different sensitivities to indoor air temperature increases. Herein, the results of two different cooling distribution scenarios were presented.

(1) Scenario 1: same indoor air temperature increase rate

As shown in Fig.9, the improved cooling distributor could make the indoor air temperature of each zone during the DR event increase to the acceptable indoor air temperature limit (i.e., 27℃) with nearly the same rate. During the power rebound period, the proposed strategy was not released until the indoor air temperature of each zone resumed to the original condition so that each zone was with the same recovery speed. Right after the power rebound period, the profiles experienced slight fluctuations caused by the handover of the control strategies after the indoor air temperature of each zone resumed to its original set-point.

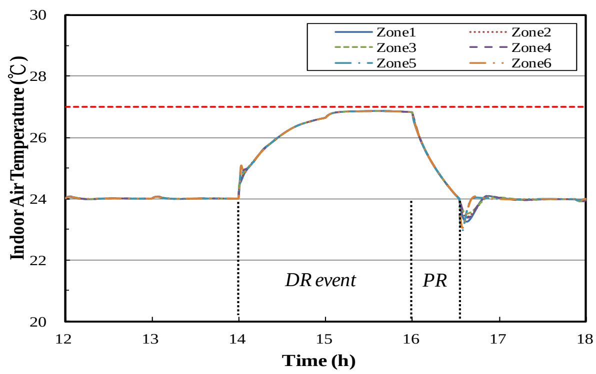

Fig.9 Temperature profiles of individual zones with same indoor air temperature increase rate during the DR event

(2) Scenario 2: different indoor air temperature increase rates

In some cases, building users prefer to have different indoor air temperature increase rates in different zones. For instance, due to the inaccurate prediction (e.g., overestimation) of the power limiting threshold, the indoor air temperature is very likely to exceed the acceptable range, which may lead to complaints by occupants. Moreover, a pre-determined power reduction during the DR event is signed ahead in the agreement in some DR programmes. In mandatory incentive-based programmes, such as Interruptible/Curtailable (I/C) service and capacity market programs (CAP), enrolled customers are subject to penalties if they do not curtail the pre-defined power reduction. In such cases, it is not economical for end-users to guarantee the indoor air temperature within the acceptable range at the expense of paying the penalty for not satisfying the pre-determined power reduction. Generally, different zones in a commercial building usually have different functions. Some zones are strict with the indoor air temperature increase while some other zones are not affected obviously even though the indoor air temperatures exceed the acceptable range. Therefore, it would be effective if different zones are with different indoor air temperature increase rates considering their individual situations. Instead of all the zones with a same increase rate, the zones, which are strict with the indoor air temperature, would be with a relatively slow increase rate. This could not only achieve a reasonable cooling distribution, but also avoid the penalty in mandatory DR programmes.

Fig.10 shows the temperature profiles of individual zones with different indoor air temperature increase rates during the DR event. The DLC strategy during the DR event was nearly the same as that in the scenario 1 and the only difference was the sensitivity of each zone to the indoor air temperature increase (i.e., the value of θ in adaptive utility function). The values of θ in zone 1 and zone 2 were set as 2, while 1.5 for the zone 3 and zone 4. The values of the other two zones were 1. As a result, the increase rates of zone 1 and zone 2 were two times compared with that of zone 5 and zone 6 while zone 3 and zone 4 were 1.5 times of that of zone 5 and 6. Zone 5 and zone 6 were the strictest with the indoor air temperature and maintained the best indoor environment during the DR event. By contrast, zone 1 and zone 2 had relatively loose requirements on the indoor air temperatures and saved the cooling supply to the others.

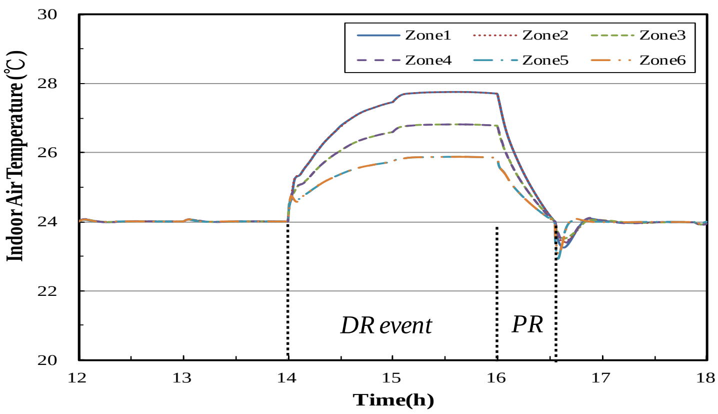

Fig.10 Temperature profiles of individual zones with different indoor air temperature increase rates during the DR event

5. Conclusions

Direct load control (DLC) by shutting down part of operating chillers in a commercial building is adopted as an effective means to respond to urgent requests of smart grids. However, no study has addressed how to determine the power limiting threshold considering an acceptable indoor air temperature increase, how to determine the numbers of chillers and pumps to be shut down and particularly how to regulate the loads of retained equipment systematically during a DR event. In this study, therefore, three schemes, i.e., building power optimization, system control resetting and online control/regulation, were developed for direct load control strategy to deal with above three issues. Under a given incentive, the building power optimization was proposed to determine the power limiting threshold considering the acceptable indoor air temperature sacrifice. The scheme of system sequence control resetting was used to determine the numbers of chillers and pumps to be retained while the scheme of online control/regulation was to make the system power demand follow the power limiting threshold by adjusting the chilled water flow rate in the secondary loop. Moreover, a modified cooling distributor was developed to effectively solve the uncertainty problem caused by the prediction process.

Test results showed that nearly 23% of immediate power reduction could be realized at the start of the DR event using the proposed DLC strategy, which was contributed by the air-conditioning system in a commercial building. With the chiller load regulator, the power consumption of the air-conditioning system could well track the command of the power limiting threshold. Two scenarios of cooling distributions were tested considering the different increase rates of indoor air temperatures. It turned out that the cooling distribution, the zones strict with the indoor air temperature increase would be with relative slow increase rates, could effectively avoid the penalty in some mandatory DR programmes. In addition, nearly 3300 kW power demand, about 34% of total power demand, could be reduced for the power grids during the power rebound period by limiting the system power consumption.

This study mainly addresses the control issues for the implementation of this fast demand response control strategy, i.e., how to control the system power demand and the cooling distribution using the supply-based feedback control strategy. However, it is worthy of noticing, for practical applications, the uncertainties need to be considered in the prediction process to improve the accuracy of prediction. The accuracy of prediction models also need to be further improved and validated before practical applications. In addition, the online control/regulation scheme in the proposed fast demand response control strategy, including the chiller load regulator and the cooling distributor, would be necessary to be tested in a real commercial building.

6. Acknowledgements

The research presented in this paper is financially supported by a grant (152152/15E) of the Research Grant Council (RGC) of the Hong Kong SAR and a grant under the Strategic Focus Area (SFA) Scheme of the Research Institute for Sustainable Urban

Development (RISUD).

References

[1] I.E. Agency. IEA Statistics: World Energy Statistice and Balances. Organisation for Economic Co-operation and Development, International Energy Agency 2014. https://www.iea.org/publications/freepublications/publication/KeyWorld2014.pdf, last viewed date: November 3, 2017.

[2] J. Kang, S.W. Wang, W.J. Gang. Performance of Distributed Energy Systems in Buildings in Cooling Dominated Regions and the Impacts of Energy Policies. Applied Thermal Engineering. (2017). doi:10.1016/j.applthermaleng.2017.08.062.

[3] K. Turitsyn, P. Sulc, S. Backhaus, M. Chertkov. Options for control of reactive power by distributed photovoltaic generators. Proceedings of the IEEE. 99 (2011) 1063-1073. doi: 10.1109/JPROC.2011.2116750.

[4] R. Allan. Reliability evaluation of power systems. Springer Science & Business Media. 2013. ISBN-10: 1489918604, ISBN-13: 9781489918604.

[5] J. Yuan, Z. Hu. Low carbon electricity development in China—An IRSP perspective based on Super Smart Grid. Renewable and Sustainable Energy Reviews. 15 (2011) 2707-2713. doi: 10.1016/j.rser.2011.02.033.

[6] M.H. Albadi, E. El-Saadany. A summary of demand response in electricity markets. Electric power systems research. 78 (2008) 1989-1996. **Error! Hyperlink reference not valid.**doi: 10.1016/j.epsr.2008.04.002.

[7] M.M. Hu, F. Xiao, L.S. Wang. Investigation of demand response potentials of residential air conditioners in smart grids using grey-box room thermal model. Applied Energy. (2017). doi: 10.1016/j.apenergy.2017.05.099.

[8] P. Pinson, H. Madsen. Benefits and challenges of electrical demand response: A critical review. Renewable and Sustainable Energy Reviews. 39 (2014) 686-699. doi: 10.1016/j.rser.2014.07.098.

[9] S.W. Wang, X. Xue, C.C. Yan. Building power demand response methods toward smart grid. HVAC&R Research. 20 (2014) 665-687. doi: 10.1080/10789669.2014.929887.

[10] J.S. Chou, N.T. Ngo. Smart grid data analytics framework for increasing energy savings in residential buildings. Automation in Construction. 72 (2016) 247-257. doi: 10.1016/j.autcon.2016.01.002.

[11] P. Palensky, D. Dietrich. Demand side management: Demand response, intelligent energy systems, and smart loads. IEEE transactions on industrial informatics. 7 (2011) 381-388. doi: 10.1109/TII.2011.2158841.

[12] L. Pérez-Lombard, J. Ortiz, C. Pout. A review on buildings energy consumption information. Energy and buildings. 40 (2008) 394-398. doi: 10.1016/j.enbuild.2007.03.007.

[13] N. Li, G. Calis, B. Becerik-Gerber. Measuring and monitoring occupancy with an RFID based system for demand-driven HVAC operations. Automation in construction. 24 (2012) 89-99. **Error! Hyperlink reference not valid.**doi: 10.1016/j.autcon.2012.02.013.

[14] A. Hajiah, M. Krarti. Optimal control of building storage systems using both ice storage and thermal mass–Part I: Simulation environment. Energy conversion and management. 64 (2012) 499-508. doi: 10.1016/j.enconman.2012.02.016.

[15] W. Turner, I. Walker, J. Roux. Peak load reductions: Electric load shifting with mechanical pre-cooling of residential buildings with low thermal mass. Energy. 82 (2015) 1057-1067. doi: 10.1016/j.energy.2015.02.011.

[16] K. Herter, P. McAuliffe, A. Rosenfeld. An exploratory analysis of California residential customer response to critical peak pricing of electricity. Energy. 32 (2007) 25-34. doi: 10.1016/j.energy.2006.01.014.

[17] F. Kuznik, J. Virgone, J.-J. Roux. Energetic efficiency of room wall containing PCM wallboard: a full-scale experimental investigation. Energy and buildings. 40 (2008) 148-156. doi: 10.1016/j.enbuild.2007.01.022.

[18] P. Xu, P. Haves, M.A. Piette, J. Braun. Peak demand reduction from pre-cooling with zone temperature reset in an office building. Lawrence Berkeley National Laboratory. (2004). http://escholarship.org/uc/item/1205612d, last viewed date: November 3, 2017.

[19] Y.J. Sun, S.W. Wang, G.S. Huang. A demand limiting strategy for maximizing monthly cost savings of commercial buildings. Energy and Buildings. 42 (2010) 2219-2230. doi: 10.1016/j.enbuild.2010.07.018.

[20] K. Antonopoulos, E. Koronaki. Effect of indoor mass on the time constant and thermal delay of buildings. International Journal of Energy Research. 24 (2000) 391-402. doi: 10.1002/(SICI)1099-114X(200004)24:5<391::AID-ER585>3.0.CO;2-L.

[21] H. Aalami, M.P. Moghaddam, G. Yousefi. Demand response modeling considering interruptible/curtailable loads and capacity market programs. Applied Energy. 87 (2010) 243-250. doi: 10.1016/j.apenergy.2009.05.041.

[22] S.W. Wang, D.C. Gao, R. Tang, F. Xiao. Cooling Supply-based HVAC System Control for Fast Demand Response of Buildings to Urgent Requests of Smart Grids. Energy Procedia. 103 (2016) 34-39. doi: 10.1016/j.egypro.2016.11.245.

[23] Y.J. Kim, L.K. Norford, J.L. Kirtley. Modeling and analysis of a variable speed heat pump for frequency regulation through direct load control. IEEE Transactions on Power Systems. 30 (2015) 397-408. doi: 10.1109/TPWRS.2014.2319310.

[24] Q. Cui, X. Wang, X. Wang, Y. Zhang. Residential appliances direct load control in real-time using cooperative game. IEEE Transactions on Power Systems. 31 (2016) 226-233. doi: 10.1109/TPWRS.2015.2391774.

[25] R. Tang, S.W. Wang, D.C. Gao, K. Shan. A power limiting control strategy based on adaptive utility function for fast demand response of buildings in smart grids. Science and Technology for the Built Environment. 22 (2016) 810-819. doi: 10.1080/23744731.2016.1198214.

[26] X. Xue, S.W. Wang, Y.J. Sun, F. Xiao. An interactive building power demand management strategy for facilitating smart grid optimization. Applied Energy. 116 (2014) 297-310. doi: 10.1016/j.apenergy.2013.11.064.

[27] B.R. Cui, D.C. Gao, S.W. Wang, X. Xue. Effectiveness and life-cycle cost-benefit analysis of active cold storages for building demand management for smart grid applications. Applied energy. 147 (2015) 523-535. doi: 10.1016/j.apenergy.2015.03.041.

[28] S.W. Wang, J. Burnett. Online adaptive control for optimizing variable-speed pumps of indirect water-cooled chilling systems. Applied Thermal Engineering. 21 (2001) 1083-1103. doi: 10.1016/S1359-4311(00)00109-5.

[29] Q. Cheng, S.W. Wang, C.C. Yan. Robust optimal design of chilled water systems in buildings with quantified uncertainty and reliability for minimized life-cycle cost. Energy and Buildings. 126 (2016) 159-169. doi: 10.1016/j.enbuild.2016.05.032.

[30] W.P. Bahnfleth, E.B. Peyer. Energy Use and Economic Comparison of Chilled-Water Pumping System Alternatives. ASHRAE transactions. 112 (2006). https://www.researchgate.net/publication/282054134_Energy_use_and_economic_comparison_of_chilled-water_pumping_system_alternatives, last viewed date: November 3, 2017.

[31] J.B. Rishel, T.H. Durkin, B.L. Kincaid, Rishel-Durkin-Kincaid. HVAC pump handbook. McGraw-HiIl 2006. ISBN-10: 0070530335, ISBN-13: 9780071457842.

[32] S.W. Wang, J. Burnett. Variable-air-volume air-conditioning systems: optimal reset of static pressure setpoint. Building Services Engineering Research and Technology. 19 (1998) 219-231. doi: 10.1177/014362449801900406.

[33] S.W. Wang, R. Tang. Supply-based feedback control strategy of air-conditioning systems for direct load control of buildings responding to urgent re

quests of smart grids. Applied Energy. 201 (2017). 419-432. doi: 10.1016/j.apenergy.2016.10.067.
[34] S.W. Wang. Dynamic simulation of a building central chilling system and evaluation of EMCS on-line control strategies. Building and Environment. 33 (1998) 1-20. doi: 10.1016/S0360-1323(97)00019-X.
[35] K. Shan, S.W. Wang, D.C. Gao, F. Xiao. Development and validation of an effective and robust chiller sequence control strategy using data-driven models. Automation in Construction. 65 (2016) 78-85. doi: 10.1016/j.autcon.2016.01.005.

Nomenclature

DR demand response
DLC direct load control
AHU air handling unit
VAV variable air volume
U utility value
Q cooling demand
M flow rate
T temperature
P power demand
PLR part load ratio
A building surface area
H pressure head
N number

Superscripts

k number of iteration

Subscripts

thr power limiting threshold
dem demand
base baseline
bui building
in indoor
ac air-conditioning
ch chiller
pri primary pump
sec secondary pump/loop
fan air delivery fan
sp set-point
tot total
w water
a air
i i^{th} zone